Task-Agnostic Exoskeleton Torque Assistance Reduces Ankle Osteoarthritis Pain: A Pilot Study

Katharine Walters, Ernesto Hernandez Hinojosa, and Robert D. Gregg

***Abstract*— Ankle osteoarthritis (OA) is a chronic joint disorder that causes significant pain and mobility challenges during activities like walking and stair navigation, where high plantarflexor torque demands exacerbate compressive loads on degraded cartilage and subchondral bone. Conventional ankle braces stabilize the joint but often immobilize it, leading to compensatory gait patterns. While powered exoskeletons could alleviate joint stress, many designs are insufficiently backdrivable or versatile to support the volitional motion of OA patients across daily activities. We address these challenges with a lightweight, backdrivable ankle exoskeleton featuring quasi-direct drive actuators and a task-agnostic control framework. This system provides continuous, biomimetic torque assistance for plantarflexion and dorsiflexion, reducing joint loads while preserving natural mobility. In pilot trials with individuals with ankle OA, our device reduced pain and peak joint torque, while improving gait symmetry, stride length, and walking speed. These results highlight the potential of backdrivable ankle exoskeletons as an innovative, non-invasive treatment for ankle OA.**

I. Introduction

Affecting approximately 1% of adults globally [1], ankle osteoarthritis (OA) is a debilitating condition characterized by progressive cartilage degradation and chronic pain exacerbated during dynamic weight-bearing activities such as walking, stair climbing and running. Ankle OA frequently stems from post-traumatic joint injuries and is less age-dependent than knee and hip OA [2]. Individuals with ankle OA frequently adopt compensatory strategies to minimize painful joint loading, including shorter strides, slower walking speed, and reductions in ankle torque [3]. While existing treatments including physical therapy and analgesics focus on pain management, they fail to address the biomechanical factors contributing to a cycle of pain, muscle weakness, and OA progression [4]. This inadequacy often necessitates invasive interventions like ankle fusion surgery, an expensive procedure with a long recovery period that permanently reduces ankle mobility [5].

The primary non-surgical treatment of ankle OA is an ankle-foot orthosis (i.e., ankle brace), where the main goal is to limit excessive joint motion and reduce stress on the affected joint surface [6], [7]. Immobilizing the joint in the neutral position is effective at reducing pain by distributing joint forces over the greatest surface area and supporting ankle instability resulting from degradation of the articular surface [8]. However, constraining ankle mobility can exacerbate gait asymmetries [9], inhibits the generation of mechanical work, and discourages active muscle engagement.

Powered ankle exoskeletons offer a promising solution for addressing the biomechanical deficits associated with ankle OA by actively assisting ankle kinetics. Partial ankle torque assistance has been shown to reduce effort [10], [11] for able-bodied users and improve gait outcomes (e.g., walking speed) for users with neurological impairments [12]–[14]. However, previous studies with powered assistance have prioritized users with structurally healthy joints, and its application for ankle OA remains unexplored. This gap is particularly notable given emerging evidence that older adults perceive exoskeletons as appealing tools for mitigating joint pain during daily activities [15], underscoring the need to evaluate their potential in populations with degenerative conditions like ankle OA.

To address this gap, we propose leveraging our lightweight, backdrivable ankle exoskeleton featuring quasi-direct drive actuation and a task-agnostic torque control framework [16]. The system continuously estimates biological joint torque demands using real-time kinematic and ground reaction force data, enabling biomimetic assistance across the entire gait cycle [17], [18]. The actuator's coaxial placement with the ankle augments the user's kinetics without applying forces on the compromised articular surfaces. This backdrivable actuation and task-agnostic control paradigm has been shown to reduce acute pain in knee and hip OA [19], [20], motivating its application to ankle OA.

This paper presents the first clinical evaluation of a powered ankle exoskeleton for mitigating pain and improving gait biomechanics in individuals with moderate-to-severe ankle OA. Preliminary results demonstrate reductions in perceived pain during assisted walking, alongside improvements in gait symmetry and walking speed. These findings suggest that biomimetic torque assistance can alleviate painful joint loading, enhance mobility, and possibly break the negative cycle of inactivity, muscle weakness, and OA progression [21]. By addressing both symptoms and biomechanical etiology, backdrivable exoskeletons could potentially offer a transformative, non-invasive solution for improving quality of life in individuals with ankle OA.

II. Methods

A. Controller Overview

We implemented a data-driven energy shaping controller for assisting plantar- and dorsi-flexion, which was previously

This work was supported by the National Institute of Biomedical Imaging and Bioengineering of the NIH under Award Number R01EB031166. The content is solely the responsibility of the authors and does not necessarily represent the official views of the NIH.

The authors are with the Department of Robotics, University of Michigan, Ann Arbor, MI 48109, USA. Contact: {kwalte, ehdz, rdgregg}@umich.edu

designed in [17] based on the framework in [16], [18]. Energy shaping control is inherently task-agnostic, as it does not enforce a specific kinematic trajectory and applies torque as a function of the instantaneous system configuration. To design a controller that generalizes across tasks and users, we formulate a convex optimization over a basis function representation of the space of possible controllers. The basis functions are trigonometric functions of the system angles, where some functions are further scaled by system angular velocities, normal ground reaction force (nGRF), or the center-of-pressure (COP). Two sets of functions separately approximate stance and swing torque, where the controller smoothly transitions between the gait phases via a low-pass filtered step function of the nGRF. The mass-normalized control torque is the convex sum of basis functions scaled by scalar coefficients. We optimize the coefficients to minimize the error between the control torque and mass-normalized reference torque across a range of tasks and subjects from a normative able-bodied dataset.

B. Hardware Implementation

The controller was implemented on a modular, backdrivable ankle exoskeleton (Figure 1), modified from [16]. Briefly, torque is applied by an actuator with a brushless DC motor and integrated 9:1 planetary gearset (T-motor AK80-9) with custom motor electronics (Dephy, MA), enabling 25Nm peak applied torque and low dynamic backdrive torque [22]. The actuator is secured to a reinforced shoe and the user's shank via two aluminum sheet-metal uprights. At the shank, torque is transferred to the user via a 3D-printed shank cuff with aluminum sheet-metal reinforcement. At the foot, torque is transferred via a carbon fiber plate embedded in the sole of a commercial boot (Dephy, MA) or an aluminum plate embedded in the sole of a modified athletic shoe. Each unilateral exoskeleton is controlled by a Raspberry Pi 5 with 8GB RAM housed in a 3D-printed electronics box on the proximal upright. Each exoskeleton is powered by a 24V, 2Ah lithium-ion battery (Kobalt), carried by the user on a waist-belt. Each unilateral exoskeleton (including the structural components, actuator, electronics, and sensor suite) weighs 1.25kg and a single US men's size 10 reinforced shoe adds 0.38kg. Each battery adds 0.64kg at the waist.

The controller runs independently on each unilateral exoskeleton, relying on a sensor suite local to each self-contained device. Inertial measurement units (IMUs) are mounted on the shank and foot to measure the global link angles and velocities (3DM-GX5-25, Lord MicroStrain). Force feedback is obtained via a pressure-sensing insole (FSR) placed under the user's foot in the shoe (Actisense, IEE, Luxembourg), enabling the approximation of nGRF and COP. The torque commanded to the actuator is the mass-normalized control torque multiplied by the user's mass and a desired assistance fraction.

C. Experimental Design

We recruited n=3 participants with pain due to chronic ankle OA (see Table I), assessed via an interview. The study

Fig. 1. Modular, backdrivable ankle exoskeleton, modified from [16]. The device can be worn unilaterally or bilaterally.

was approved by the University of Michigan's Institutional Review Board (HUM00201957). The study assessed subjective pain, plantar- and dorsi-flexor muscle activity, ankle kinetics, and spatiotemporal gait parameters for treadmill ambulation tasks without the exo (Bare) and with the exo powered (Exo). Participant P1 wore reinforced boots, as the calf-height laces emulated the compression effect of their standard-of-care compression brace. Participants P2 and P3 wore reinforced athletic shoes as they did not have a standard-of-care brace. Participants wore the exo on their affected side(s) (see Table I) and wore the same reinforced footwear bilaterally for the Bare and Exo conditions.

TABLE I
SUBJECT INFORMATION

	Sex	Age	Weight (kg)	Height (m)	Affected Side
P1	F	65	64	1.70	L & R
P2	M	73	84.5	1.85	R
P3	F	65	75.7	1.57	L

Before data collection, participants selected their preferred level, incline, and decline treadmill walking speeds via a GUI. The preferred walking speeds for participants P1, P2, and P3 were respectively 0.8, 0.65, and 0.7 m/s for level ground, 0.7, 0.45, and 0.7 m/s for incline, and 0.6, 0.55, and 0.6 m/s for decline walking. Each selected speed was fixed for both Bare and Exo conditions. Participants then donned the exoskeleton and acclimated under increasing assistance fractions until they were confident with the device and the assistance saturated at the peak device torque. To investigate the effect of varying levels of assistance (LoAs), the assistance fraction achieving peak device torque is designated as "high" LoA, and 40% and 70% of peak torque are designated as "low" and "med" (medium), respectively.

The experiment tasks included level, 10° incline, and 10° decline walking, as well as a six-minute walk test (6MWT). All tasks were performed on a split-belt force-instrumented treadmill (Bertec, OH) in a single session. The level, incline, and decline walking tasks were 3 minutes in duration for Bare and Exo conditions, where each minute of the Exo condition had a different LoA (low, med, high). Participants

were asked to verbally report their pain in the affected ankle(s) after each minute. For the 6MWT, participants were instructed to walk as far as comfortably possible on a level treadmill and were able to continually adjust the treadmill speed using the GUI. Participants were asked to report their pain after the conclusion of the 6MWT. The Exo 6MWT applied high assistance for the duration of the test. The order of Bare and Exo conditions and the order of LoA within the Exo condition were randomized between participants.

D. Data Collection and Analysis

Pain was verbally assessed using the Numeric Pain Scale on a scale of 0-10, where 0 indicated no pain and 10 indicated the worst pain [23]. Muscle effort was assessed using surface electromyography (EMG). After appropriate skin preparation, we taped four wireless electrodes (Delsys, Massachusetts, USA) onto the participant's affected lower limb over the lateral gastrocnemius, medial gastrocnemius, soleus, and tibialis anterior to assess muscle activation. EMG data was parsed into individual task/gait cycles using the ground reaction force from the Bertec forceplates. Each muscle's EMG was demeaned, bandpass filtered (20 - 200 Hz), and smoothed with a moving 125 ms window RMS filter with 50% overlap. EMG was normalized to the maximum muscle activation level observed during the test. We then calculated the mean and peak muscle activation for each muscle, taking the difference between the Exo and Bare conditions. Specifically, the peak EMG difference for each muscle/activity was calculated by normalizing the peak EMG of each trial in the Exo condition relative to the Bare condition, using the formula

$$\text{Normalized Peak EMG} = \frac{\text{Exo Peak} - \text{Bare Peak}}{\text{Bare Peak}}.$$

Finally, the four muscles were lumped together using a weighted average based on each muscle's cross-sectional area to acquire the overall mean and peak activations for each activity.

Ankle kinematics were assessed via motion capture at 250Hz (Vicon, NY) and ground reaction forces were collected from the Bertec forceplates at 2000Hz. As we were interested only in outcomes local to the ankle, we placed a limited marker set bilaterally, with markers on the 1st, 3rd, and 5th metacarpals, the heel, distal and proximal tibia markers, medial and lateral knee markers, and two markers on the thigh. The thigh markers were disregarded in analysis. A static bare trial included medial and lateral ankle markers. As the lateral ankle was obscured by the actuator during the Exo trials, the medial and lateral ankle positions were calculated in post-processing via a rigid body transformation relative to the knee and tibia markers. The ankle angle was calculated as the angle between a vector normal to the shank and a vector normal to the foot. As ankle torque is significantly higher during stance than swing, we neglected kinetics during swing. We calculated stance ankle torque as the cross-product between a vector from the ankle joint center to the center of pressure and the force vector, transformed to the sagittal plane. In the Exo condition, we subtracted the applied exo torque from the calculated net ankle torque to find the human ankle torque.

We assessed stance symmetry and stride length for the level, incline, and decline walking tasks, where strides are defined heelstrike to heelstrike. We calculated stance symmetry by comparing the stance duration as a percentage of the stride between the left and right legs using the symmetry index (SI),

$$SI = \frac{|X_L - X_R|}{0.5(|X_L| + |X_R|)} \times 100,$$

where 0 indicates perfect symmetry [24]. The stride length was calculated by multiplying the stride duration by the treadmill speed, where the stride duration was averaged across the left and right legs as there was negligible stride duration asymmetry for all participants.

III. Results

A. Pain Reductions

Figure 2 illustrates participants' perceived pain score reductions during level, incline and decline walking with low, medium and high assistance levels, as well as the pain score reduction during the 6MWT. P1 experienced the greatest pain reduction on the left ankle during incline walking with high assistance, as well as during decline walking with medium and high assistance (a reduction of two points in all cases). On the right ankle, the greatest pain reduction was a one-point reduction observed during level walking with high assistance, incline walking with all three assistance levels, and decline walking with high assistance. On average, P1 experienced a pain reduction of 0.78 points on the left ankle and 0.56 points on the right ankle. P2 exhibited the largest overall pain reductions during incline walking, with reductions of 4, 2, and 3 points for low, medium, and high assistance levels, respectively. On average, P2 experienced a pain reduction of 1.56 points. P3 reported the largest pain reduction during decline walking with low assistance, observing a two-point reduction. On average, P3 experienced a pain reduction of 0.67 points across all tasks. Across all participants, tasks, and assistance levels, the overall average pain reduction was 0.89 points. When considering only trials with high assistance, the overall average pain reduction was 1.13 points. In the 6MWT, the average pain reduction was 1.5 points with P2 and P3 each having reduction of 2 points.

Figure 3 illustrates the average effect of walking time on perceived pain. Longitudinal analysis using three separate mixed-effects models (one for each task) revealed distinct pain progression patterns between exo-assisted and bare walking. In the Bare condition, the task-specific models demonstrated a consistent positive association between walking duration and pain intensity (slope coefficients: 0.125 to 0.375; conditional R^2 = 0.72 to 0.97), with the strongest effects observed during decline walking (conditional $R^2 = 0.97$). Conversely, exoskeleton use attenuated these trends, yielding negative slopes (slope coefficients: -0.1125 to -0.25; conditional R^2 = 0.32 to 0.91).

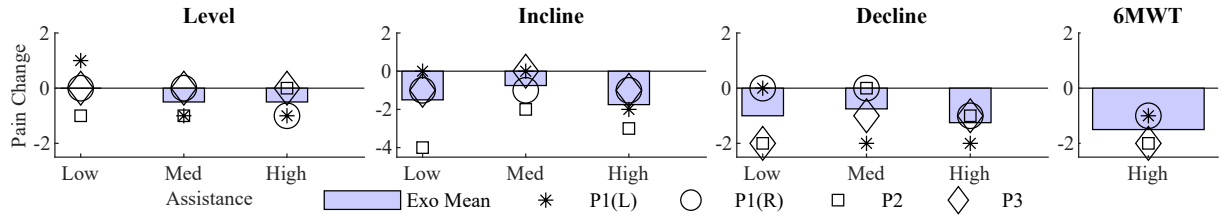

Fig. 2. Changes in perceived pain scores compared to bare walking during level, incline, and decline walking at low, medium, and high assistance levels. The 6MWT was conducted exclusively at high assistance. Mean values and individual data points illustrate the variability in pain responses, highlighting task- and participant-specific effects of exoskeleton assistance.

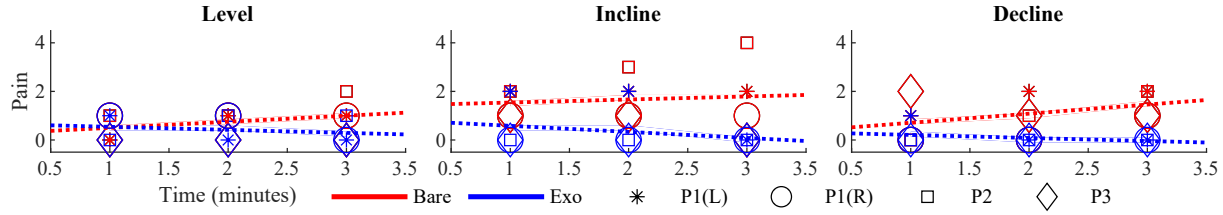

Fig. 3. Perceived pain scores during level, incline, and decline walking over time. The dotted lines represent the best-fit trend lines for the pain scores in the bare (red) and exoskeleton (blue) conditions as a function of walking time. The data suggest a tendency for pain to increase over time during the bare condition, while it decreases during the exoskeleton-assisted condition.

B. Muscle Activity

Table II summarizes changes in peak EMG activation across participants. P1 demonstrated a reduction in peak activation in the right leg during level and incline walking, with an average change of -3.2%. In contrast, the left leg of P1 exhibited an increase in peak activation, averaging +43.3%. P2 showed reductions in peak activation across all tasks, with an overall average change of -34.1%. The largest reduction occurred during level walking (-50.5%). P3 experienced increased peak activation across all tasks, with an average change of +19.3%. Overall, peak EMG activation was reduced in P1(R) and P2, with a combined average reduction of -18.7% but increased for P1(L) and P3, indicating individual variability in muscle response to exoskeleton assistance with limited acclimation time.

TABLE II

PEAK EMG DIFFERENCE (% CHANGE RELATIVE TO BARE)

	Level	Incline	Decline	Avg.
P1(L)	68.7	17.8	–	43.3
P1(R)	**-1.0**	**-5.4**	–	**-3.2**
P2	**-50.5**	**-6.1**	**-36.0**	**-34.1**
P3	31.0	13.9	23.2	19.3
Avg.	9.8	6.8	**-6.4**	6.3

C. Spatiotemporal Gait Parameters

Table III summarizes how high exo assistance affected self-selected walking speeds during the 6MWT. The impact varied notably among participants. While P1's speeds decreased with the exo, showing a 7.54% reduction in mean speed and an 8.83% reduction in maximum speed, both P2 and P3 achieved substantial improvements. P2 increased their mean speed by 17.75% and maximum speed by 25.03%, while P3 demonstrated the most dramatic improvements with a 34.41% increase in mean speed and a 60.05% increase in maximum speed. Collectively, participants showed an overall improvement of 14.87% in mean speed and 25.42% in maximum speed.

TABLE III

SIX-MINUTE WALK TEST SELECTED WALKING SPEEDS

	Bare Max (m/s)	Exo Max (m/s)	Change (%)	Bare Mean (m/s)	Exo Mean (m/s)	Change (%)
P1	1.7	1.55	-8.83	1.53	1.41	-7.54
P2	0.8	1	**25.03**	0.73	0.86	**17.75**
P3	0.75	1.2	**60.05**	0.7	0.94	**34.41**
Avg.	1.08	1.25	**25.42**	0.99	1.07	**14.87**

Figure 4 summarizes how high exo assistance affected stance symmetry index (SI) and stride length compared to bare. During level walking, stance SI changes were minimal, with an average change of -0.1% and all participants showing modest variations of less than 2%. The exo's impact on symmetry became more pronounced during non-level walking, with all participants showing improved symmetry (positive SI reductions) during both incline and decline conditions. Incline walking yielded an average SI reduction of 1.6%, ranging from 0.4% for P2 to 3.4% for P3. The most substantial improvements occurred during decline walking, with an average reduction of 2.5% and P1 achieving a notable 6.5% reduction. Across all walking conditions, participants experienced an average stance SI reduction of 1.3%.

The exo generally enabled participants to walk with longer stride lengths across all walking conditions. Level walking yielded an average stride length increase of 2.9%, though individual responses varied considerably, from a 3.9% decrease for P3 to a 7.7% increase for P2. During incline walking, the average stride length increased by 2%, with P1 and P2 showing similar improvements of 3.3% and 3.6% respectively, while P3 had a minimal change of -0.8%. The most substantial improvements occurred during decline walking, where participants averaged a 4.9% increase in stride length, with P1 achieving the largest individual improvement of 8.5%. Across all walking conditions, participants demonstrated an overall average increase in stride length of 3.3%.

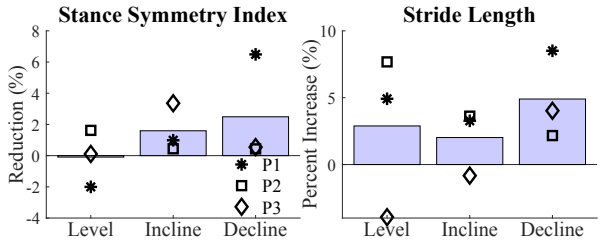

Fig. 4. Change in stance symmetry index and stride length for high exo assistance compared to bare for level, incline, and decline walking. Bars indicate inter-subject averages and scatter points indicate intra-subject averages. A positive reduction in stance symmetry index indicates a symmetry improvement for Exo compared to Bare.

D. Torque and Power Reductions

Figure 5 demonstrates the effect of high exo assistance on biological ankle torque and power. On the affected side, the exo applied torque that closely matched natural biomimetic patterns, enabling participants to reduce their own torque contribution. This assistance led to reductions in both average peak positive power and the magnitude of peak negative power compared to bare.

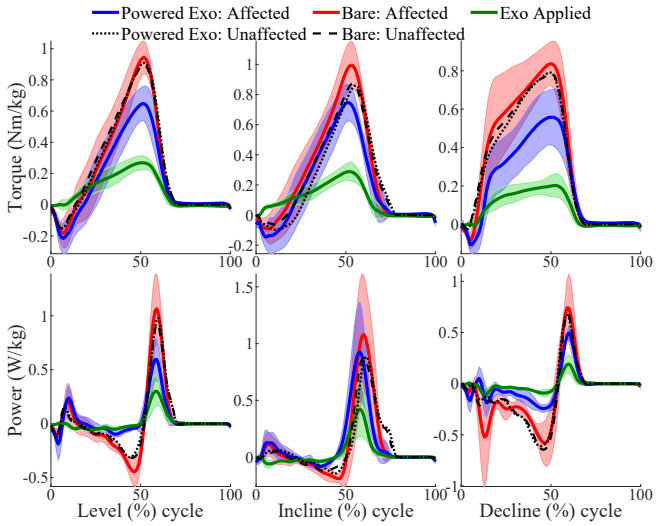

Fig. 5. Inter-subject, mass-normalized average (solid) and standard deviation (shaded) torque and power for the assisted (blue) ankle during high assistance and bare (red) ankle affected by OA pain. The inter-subject, mass-normalized applied exoskeleton assistance is shown in green. The affected ankle shows reduced peak torque and peak positive power with the exo assistance across all tasks. The inter-subject mean torque and power for the unaffected side during the exo condition (black dotted) and bare condition (black dashed) overlap, illustrating a lack of significant compensations on the unaffected side.

Peak torque and peak power reductions varied notably across participants and walking conditions, as detailed in Tables IV and V, respectively. All participants experienced peak torque reductions across all tasks. P2 exhibited more modest improvements, with the smallest task-specific peak torque reduction of 11.6% during incline walking and the lowest overall reduction of 18% across tasks. In contrast, P1 achieved the most substantial improvements, with a 42.8% peak torque reduction on their right side during level walking and the highest overall reduction of 44.2% on their right side. Similarly, peak power reductions were observed in most conditions, with P1 achieving the most substantial reduction of 61.2% during decline walking. The only exception was P2, who showed a slight 2% increase during decline walking. Across all tasks, participants averaged a 29.6% reduction in peak ankle torque and a 30.3% reduction in peak positive power on their affected side.

TABLE IV
PEAK TORQUE DIFFERENCE WITH HIGH ASSISTANCE
(% CHANGE RELATIVE TO BARE)

	Level	Incline	Decline	Avg.
P1(L)	**-15.4**	**-20.9**	**-32.5**	**-22.9**
P1(R)	**-42.8**	**-36.7**	**-53**	**-44.2**
P2	**-29.8**	**-11.6**	**-12.7**	**-18**
P3	**-35.9**	**-30.2**	**-33.4**	**-33.2**
Avg.	**-31**	**-24.9**	**-32.9**	**-29.6**

TABLE V
PEAK POSITIVE POWER DIFFERENCE WITH HIGH ASSISTANCE
(% CHANGE RELATIVE TO BARE)

	Level	Incline	Decline	Avg.
P1(L)	**-28.9**	**-12.2**	**-28.8**	**-23.3**
P1(R)	**-53.4**	**-25.6**	**-61.2**	**-46.7**
P2	**-41.6**	**-12**	2	**-17.2**
P3	**-40.9**	**-19.3**	**-42.2**	**-34.1**
Avg.	**-41.2**	**-17.3**	**-32.6**	**-30.3**

IV. DISCUSSION

Our study demonstrates that the powered ankle exoskeleton assistance provides immediate benefits for individuals with ankle OA by effectively reducing pain levels across various walking scenarios. As opposed to traditional braces that support the ankle while limiting joint motion, our exoskeleton employs a task-agnostic, biomimetic torque assistance paradigm to dynamically support joint motion throughout the gait cycle. By prioritizing both pain relief and functional mobility, this approach presents a novel pathway to enhancing quality of life for individuals with ankle OA.

A. Pain Reductions

The 6MWT and incline walking with high assistance both demonstrated the highest pain reduction, with an average decrease of 1.5 points across participants. For the 6MWT, this outcome is likely attributable to the task's extended duration (6 minutes vs. 3 minutes for other tasks) and the heightened physical effort required, as participants were instructed to maximize distance rather than maintain a self-selected pace. In contrast, the pain reduction during incline walking with high assistance may be attributed to the increased demands on the plantarflexors to propel the body against gravity. The uphill motion requires greater joint flexion and extension, leading to elevated compressive forces on the inflamed joint surfaces. By providing targeted assistance, the exoskeleton likely mitigates some of these compressive forces by reducing the muscular effort required for proper motion, thereby contributing to the observed pain relief. Level walking exhibited only slight pain reduction, which can likely be attributed to the lower baseline pain

levels generally associated with this activity and its relatively lower demand for muscle engagement.

The data revealed a positive correlation between pain and time spent walking across all tasks and participants without exoskeleton assistance. This observation aligns with prior research suggesting that ankle OA pain may increase over time as degraded cartilage and weakened muscles/tendons exacerbate stress on the joint, heightening nociceptive signaling and intensifying pain over time [25], [26]. On the other hand, with exoskeleton assistance, a negative correlation between pain and walking duration was observed across all tasks and participants. These results preliminarily indicate that extended unassisted walking exacerbates pain across terrains, whereas exoskeleton integration may counteract this effect, warranting validation in larger cohorts to establish robustness and generalize findings.

B. Muscle Activity

The peak EMG differences across participants showed some notable trends. Despite having the same exoskeleton assistance applied to both sides, P1 exhibited a decrease in peak EMG for the right ankle but an increase for the left ankle during level and incline walking. P2 had reductions in peak EMG for all walking tasks, whereas P3 showed the opposite. On average, only P1(R) and P2 exhibited a reduction in peak EMG, resulting in an overall increase of 6.3% across all participants and tasks. These results suggest that muscle effort alone cannot explain the consistent pain reductions experienced by all participants.

This discrepancy might be explained by individual differences in adaptation to the device, muscle coordination, and the specific demands of each task. Participants who exhibited reductions in peak EMG (P2) may have better adapted to the exoskeleton, resulting in less muscle effort to achieve the same task. Conversely, those with increased peak EMG (P1(L) and P3) might not have fully acclimated to the device or might have experienced compensatory muscle activation in response to the exoskeleton's assistance. Previous studies have suggested that acclimatization to exoskeletons, especially in older or clinical populations, may require longer periods of use before consistent reductions in metabolic cost are observed [27], [28]. Additionally, it is possible that pain reduction, particularly in individuals with OA, could lead to greater mobility and less guarded movement, which may not necessarily correlate with reduced muscle activation with respect to baseline in all cases.

C. Spatiotemporal Gait Parameters

The trends of increased walking speed, improved stance symmetry, and longer stride length suggest that exo assistance has the potential to mitigate mobility reductions associated with painful OA joint loading, which include decreased velocity and stride length [3]. However, benefits related to walking speed appear to depend on baseline mobility levels. P1 exhibited "high mobility" with a mean self-selected bare walking speed of 1.53 m/s during the 6MWT, while P2 and P3 showed "low mobility" with speeds of 0.73 m/s and 0.7 m/s, respectively. For P1, higher accelerations yielded larger inertial penalties from the added device mass and backdrive torque, likely contributing to a reduced self-selected speed. In contrast, P2 and P3 achieved substantially higher speeds with the exo, likely due to slower baseline mobility and smaller inertial penalties. Notably, all participants had reduced pain with the exo, suggesting that active assistance could encourage OA patients to engage in faster and/or longer periods of walking and benefit overall health.

Despite inter-subject and inter-task variation, improvements in stride length and stance symmetry are notable due to the inertial penalties of wearing the device. Longer strides are likely the result of reduced pain and indicate confidence with the device. Further, improved symmetry is meaningful for reducing gait compensations that could lead to secondary musculoskeletal issues. Interestingly, P1 was the only participant wearing bilateral exos, and they were also the only participant exhibiting a negative impact on stance symmetry.

D. Torque and Power Reductions

The exoskeleton's biomimetic torque assistance consistently reduced the affected-ankle torque contribution without compensatory loading of the unaffected ankle. Reductions in joint torque are linked to reductions in painful compressive loading of the joint's articular surface [3], [29], [30]. This may explain why our OA participants' 29.6% average torque reduction is larger than the 18.1% average reduction observed with able-bodied participants using the same device and controller across the same tasks [17]—OA participants may adapt more quickly or fully to the assistance due to the immediate pain relief associated with decreased torque-related joint loading.

In addition to peak positive power reductions across tasks, participants also exhibited fairly substantial reductions in negative power magnitudes with biomimetic assistance. Though previous work has suggested that this outcome is not energetically optimal for able-bodied participants [31], it is likely that reducing negative power contributes to overall pain reduction as eccentric contractions produce larger muscle forces than concentric contractions for equivalent angular velocities [32]. Overall, it suggests that biomimetic assistance is effective for pain reduction.

E. Study Limitations and Future Work

In this study, we wanted to evaluate the effect of varying assistance levels on pain reductions and gait outcomes, so we varied the exo assistance fraction in each minute of walking. To limit the total experiment time and pain experienced by our participants, we did not evaluate a passive exo condition. However, some participants noted that the passive structure of the exoskeleton provided a stabilizing bracing effect that could have provided some pain relief. Future work should include a passive condition to isolate these effects.

With promising reductions in perceived pain across tasks and subjects, this study motivates further investigation into the mechanisms of this pain reduction. Despite showing the

least reduction in peak torque and peak power, P2 was the only participant with consistent peak EMG reductions across tasks and reported the largest overall pain reduction. However, all participants experienced average pain reductions across all tasks despite varied peak EMG differences, suggesting that perceived pain reduction is not simply explained by changes in kinetics or surface EMG. Further, given our small sample size, we can only comment on observed trends. Future work with a larger population will be necessary to explore these complex interactions between perceived pain, joint biomechanics, and gait outcomes.

V. Conclusion

This study highlights the potential of backdrivable ankle exoskeletons to deliver immediate pain relief during walking by reducing peak joint torque while improving gait metrics including symmetry, stride length, and walking speed. Although a direct causal link between reduced muscle activation and pain relief remains unconfirmed, the findings suggest that the exoskeleton enables users to perform previously painful activities with greater comfort. This device could encourage individuals with OA to increase their activity levels to promote muscle strengthening and potentially decelerate OA progression. Consequently, backdrivable exoskeletons offer a promising non-invasive solution for managing ankle OA, with the potential to enhance mobility and improve patient quality of life. Future studies with larger participant cohorts are essential to confirm and extend these findings.

References

[1] M. Herrera-Pérez, D. González-Martín, M. Vallejo-Márquez, A. L. Godoy-Santos, V. Valderrabano, and S. Tejero, "Ankle Osteoarthritis Aetiology," *J. Clin. Med.*, vol. 10, no. 19, p. 4489, 2021.

[2] A. J. Goldberg, A. MacGregor, J. Dawson, D. Singh, N. Cullen, R. J. Sharp, and P. H. Cooke, "The demand incidence of symptomatic ankle osteoarthritis presenting to foot & ankle surgeons in the United Kingdom," *The Foot*, vol. 22, no. 3, pp. 163–166, 2012.

[3] V. Valderrabano, B. M. Nigg, V. Von Tscharner, D. J. Stefanyshyn, B. Goepfert, and B. Hintermann, "Gait analysis in ankle osteoarthritis and total ankle replacement," *Clin. Biomech.*, vol. 22, no. 8, pp. 894–904, 2007.

[4] S. Tejero, E. Prada-Chamorro, D. González-Martín, A. García-Guirao, A. Galhoum, V. Valderrabano, and M. Herrera-Pérez, "Conservative Treatment of Ankle Osteoarthritis," *J. Clin. Med.*, vol. 10, no. 19, p. 4561, 2021.

[5] F.-I. Rohlfing, U. Wiebking, P. F. O'LOUGHLIN, C. Krettek, and R. Gaulke, "Clinical and radiological mid-to-long-term outcomes following ankle arthrolysis," *in vivo*, vol. 33, no. 2, pp. 535–542, 2019.

[6] M. S. Rockett, A. Ng, and M. Guimet, "Posttraumatic ankle arthrosis," *Clin. Podiatr. Med. Sur.*, vol. 18, no. 3, pp. 515–535, 2001.

[7] C. M. Bono and W. S. Berberian, "Orthotic devices. degenerative disorders of the foot and ankle." *Foot and Ankle Clinics*, vol. 6, no. 2, pp. 329–340, 2001.

[8] J. T. Deland, G. D. Morris, and I.-H. Sung, "Biomechanics of the ankle joint: A perspective on total ankle replacement," *Foot and ankle clinics*, vol. 5, no. 4, pp. 747–759, 2000.

[9] D. J. Keene, K. Willett, and S. E. Lamb, "The effects of ankle supports on gait in adults: A randomized cross-over study," *J. Electromyography and Kinesiology*, vol. 25, no. 6, pp. 973–981, 2015.

[10] L. M. Mooney, E. J. Rouse, and H. M. Herr, "Autonomous exoskeleton reduces metabolic cost of human walking during load carriage," *J NeuroEngineering Rehabil*, vol. 11, no. 1, pp. 1–11, 2014.

[11] M. B. Yandell, J. R. Tacca, and K. E. Zelik, "Design of a low profile, unpowered ankle exoskeleton that fits under clothes: overcoming practical barriers to widespread societal adoption," *IEEE Trans Neural Syst Rehabil Eng*, vol. 27, no. 4, pp. 712–723, 2019.

[12] E. A. Tagoe, Y. Fang, J. R. Williams, and Z. F. Lerner, "Walking on real-world terrain with an ankle exoskeleton in cerebral palsy," *IEEE Trans. Med. Robot. Bion.*, 2023.

[13] L.-F. Yeung, C. Ockenfeld, M.-K. Pang, H.-W. Wai, O.-Y. Soo, S.-W. Li, and K.-Y. Tong, "Design of an exoskeleton ankle robot for robot-assisted gait training of stroke patients," in *Int. Conf. Rehabil. Robot.*, 2017, pp. 211–215.

[14] K. Nakagawa, M. Tomoi, K. Higashi, S. Utsumi, R. Kawano, E. Tanaka, K. Kurisu, and L. Yuge, "Short-term effect of a close-fitting type of walking assistive device on spinal cord reciprocal inhibition," *J. Clin. Neuroscience*, vol. 77, pp. 142–147, 2020.

[15] M. Raitor, S. Ruggles, S. L. Delp, C. K. Liu, and S. H. Collins, "Lower-limb exoskeletons appeal to both clinicians and older adults, especially for fall prevention and joint pain reduction," *IEEE Trans. Neural Syst. Rehabil. Eng.*, 2024.

[16] S. Zhao, K. Walters, J. M. Pérez, and R. D. Gregg, "Design and Validation of a Modular, Backdrivable Ankle Exoskeleton," in *IEEE Int Conf Biomed Robot Biomechatron*, 2024, pp. 1454–1460.

[17] K. Walters, G. C. Thomas, and R. D. Gregg, "Optimal energy shaping and force amplification framework for task-agnostic, biomimetic ankle exoskeletons," 2025, unpublished.

[18] J. Lin, G. C. Thomas, N. V. Divekar, V. Peddinti, and R. D. Gregg, "A modular framework for task-agnostic, energy shaping control of lower limb exoskeletons," *IEEE Trans. Control Syst. Technol.*, 2024.

[19] N. Divekar, E. Hernandez Hinojosa, J. Zhang, and R. D. Gregg, "A task-agnostic knee exoskeleton for reducing osteoarthritis pain across activities of daily life: A pilot study," in *IEEE Int. Conf. on Rehab. Robotics*, 2025.

[20] J. Zhang, N. Divekar, E. Hernandez Hinojosa, and R. D. Gregg, "A task-agnostic hip exoskeleton for osteoarthritis pain relief: Energetic control across activities of daily life," in *IEEE Int. Conf. on Rehab. Robotics*, 2025.

[21] J. Dekker, P. Tola, G. Aufdemkampe, and M. Winckers, "Negative affect, pain and disability in osteoarthritis patients: the mediating role of muscle weakness," *Behaviour research and therapy*, vol. 31, no. 2, pp. 203–206, 1993.

[22] C. Nesler, G. Thomas, N. Divekar, E. J. Rouse, and R. D. Gregg, "Enhancing voluntary motion with modular, backdrivable, powered hip and knee orthoses," *IEEE Robot. Autom. Lett.*, vol. 7, no. 3, pp. 6155–6162, 2022.

[23] A. Williamson and B. Hoggart, "Pain: a review of three commonly used pain rating scales," *J. Clin. Nursing*, vol. 14, no. 7, pp. 798–804, 2005.

[24] E. Giannakou, S. Fotiadou, V. Gourgoulis, G. Mavrommatis, and N. Aggelousis, "A Comparative Analysis of Symmetry Indices for Spatiotemporal Gait Features in Early Parkinson's Disease," *Neurology International*, vol. 15, no. 3, pp. 1129–1139, 2023.

[25] H. Nie, L. Arendt-Nielsen, H. Andersen, and T. Graven-Nielsen, "Temporal Summation of Pain Evoked by Mechanical Stimulation in Deep and Superficial Tissue," *J. Pain*, vol. 6, no. 6, pp. 348–355, 2005.

[26] S. Lee, T. Neogi, K. E. Costello, B. Senderling, J. J. Stefanik, L. Frey-Law, and D. Kumar, "Association of mechanical temporal summation of pain with muscle co-contraction during walking in people with knee osteoarthritis," *Clin. Biomech.*, vol. 110, p. 106105, 2023.

[27] A. Lakmazaheri, S. Song, B. B. Vuong, B. Biskner, D. M. Kado, and S. H. Collins, "Optimizing exoskeleton assistance to improve walking speed and energy economy for older adults," *J. Neuroeng. Rehabil.*, vol. 21, no. 1, p. 1, 2024.

[28] K. L. Poggensee and S. H. Collins, "How adaptation, training, and customization contribute to benefits from exoskeleton assistance," *Science Robotics*, vol. 6, no. 58, p. eabf1078, 2021.

[29] B. J. McLain, D. Lee, S. C. Mulrine, and A. J. Young, "Effect of assistance using a bilateral robotic knee exoskeleton on tibiofemoral force using a neuromuscular model," *Annals of Biomedical Engineering*, vol. 50, no. 6, pp. 716–727, 2022.

[30] M. Praagman, M. Stokdijk, H. Veeger, and B. Visser, "Predicting mechanical load of the glenohumeral joint, using net joint moments," *Clinical biomechanics*, vol. 15, no. 5, pp. 315–321, 2000.

[31] S. Galle, P. Malcolm, S. H. Collins, and D. De Clercq, "Reducing the metabolic cost of walking with an ankle exoskeleton: interaction between actuation timing and power," *J. Neuroeng. Rehabil.*, vol. 14, no. 1, p. 35, 2017.

[32] S. Hody, J.-L. Croisier, T. Bury, B. Rogister, and P. Leprince, "Eccentric Muscle Contractions: Risks and Benefits," *Frontiers in Physiology*, vol. 10, 2019.